AJNR

Cavernous Sinus and Inferior Petrosal Sinus Flow Signal on Three-Dimensional Time-of-Flight MR Angiography

Serge Ouanounou, Thomas A. Tomsick, Charles Heitsman and Christy K. Holland

AJNR Am J Neuroradiol 1999, 20 (8) 1476-1481
http://www.ajnr.org/content/20/8/1476

AJNR Am J Neuroradiol 20:1476–1481, September 1999

Cavernous Sinus and Inferior Petrosal Sinus Flow Signal on Three-Dimensional Time-of-Flight MR Angiography

Serge Ouanounou, Thomas A. Tomsick, Charles Heitsman, and Christy K. Holland

BACKGROUND AND PURPOSE: **Venous flow signal in the cavernous sinus and inferior petrosal sinus has been shown on MR angiograms in patients with carotid cavernous fistula (CCF). We, however, identified flow signal in some patients without symptoms and signs of CCF. This review was performed to determine the frequency of such normal venous flow depiction at MR angiography.**

METHODS: **Twenty-five 3D time-of-flight (TOF) MR angiograms obtained on two different imaging units (scanners A and B) were reviewed with attention to presence of venous flow signal in the cavernous sinus or inferior petrosal sinus or both. Twenty-five additional MR angiograms were reviewed in patients who had also had cerebral arteriography to document absence of CCF where venous MR angiographic signal was detected, as well as to gain insight into venous flow patterns that might contribute to MR angiographic venous flow signal. Differences in scanning technique parameters were reviewed.**

RESULTS: **Nine (36%) of the 25 MR angiograms obtained on scanner A but only one (4%) of the 25 obtained on scanner B showed flow signal in the cavernous or inferior petrosal sinus or both in the absence of signs of CCF. On review of 25 patients who had both MR angiography and arteriography, three patients with venous signal at MR angiography failed to exhibit CCF at arteriography.**

CONCLUSION: **Identification of normal cavernous sinus or inferior petrosal sinus venous signal on 3D TOF MR angiograms may occur frequently, and is probably dependent on technical factors that vary among scanners. The exact factors most responsible, however, were not elucidated by this preliminary review.**

Several reports have been published concerning the role of MR angiography in demonstrating the abnormal venous flow of carotid cavernous fistulas (CCFs) (1–3). Cornelius (4) summarized the MR angiographic characteristics of CCF, visualizing the draining veins that commonly include the cavernous sinus, the inferior petrosal sinus, the superior petrosal sinus, the superior ophthalmic vein and sphenoparietal sinus, and the sylvian veins. A recently published study reported a sensitivity and specificity of 83% and 100%, respectively, for MR angiography in the detection of CCF (5). In addition, MR angiography may prove to be useful in following up patients treated for CCF.

It has been our experience, however, that visualization of cavernous sinus and inferior petrosal sinus flow signal may occur in uninvolved patients on routine 3D time-of-flight (TOF) MR angiographic studies (Figs 1–3). These and other similar cases prompted us to investigate the prevalence of normal flow signal in the cavernous sinus and inferior petrosal sinus on 3D TOF MR angiograms in patients without signs or symptoms of CCF.

Received September 28, 1998; accepted after revision March 29, 1999.

From the Department of Radiology, Section of Neuroradiology, University Hospital, 234 Goodman St, ML 0742, Cincinnati, OH 45219.

Address reprint requests to Thomas A. Tomsick, MD.

Methods

Fifty randomly selected MR angiographic studies performed in adult patients between June 1996 and March 1997 were evaluated for flow signal in the cavernous sinus and inferior petrosal sinus. An equal number (n = 25) of MR angiographic studies were performed using each of two 1.5-T MR instruments, designated scanner A and scanner B. Technical scanning factors are outlined in the Table 1. Both source and maximum intensity pixel reprojection (MIP) images were analyzed for flow signal in the cavernous sinus and inferior petrosal sinus. A subjective grade of 1 to 3 was given for the magnitude of any signal in either sinus: grade 1 was above background signal on reprojected images, grade 3 signal was equal to that from arterial structures of the same size, and grade 2 was intermediate signal. For each case in which signal was detected, the spin-echo (SE) MR examinations were also reviewed for any abnormality in the cavernous sinus/inferior petrosal sinus. Information concerning the patient's history, MR instrument used, sequence parameters, and multiple overlapping thin-section acquisition centering position was also noted.

Subsequently, 25 additional patients who had both MR angiography and cerebral angiography between August 1995 and

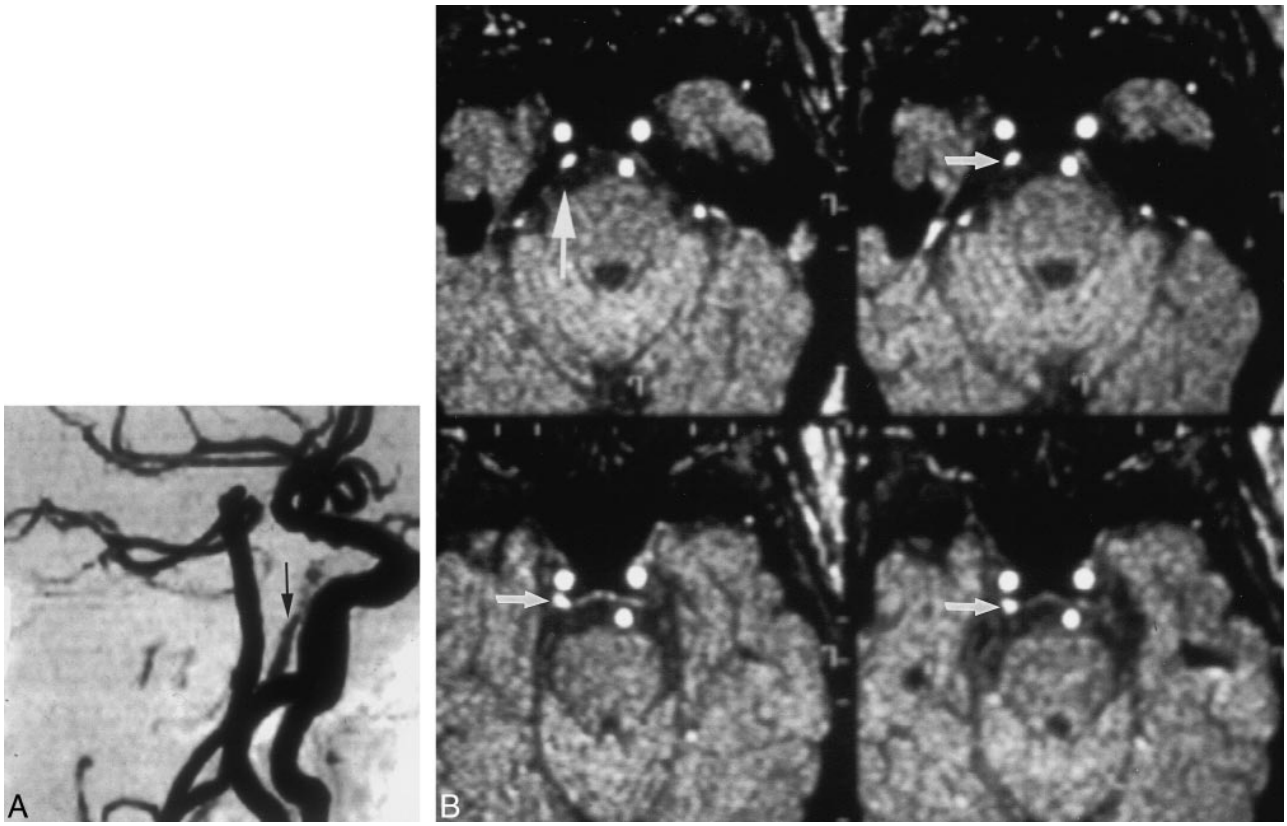

FIG 1. *A* and *B*, 3D TOF MR angiograms (42/6.9) show grade 2 posterior cavernous sinus signal and grade 3 inferior petrosal sinus signal on both MIP (*A, arrows*) and source (*B, arrows*) images.

February 1997, with no evidence of CCF, were identified and the MR angiograms reviewed in the same manner. The cerebral angiogram was reviewed only if flow signal in the cavernous sinus/inferior petrosal sinus was identified at MR angiography.

Results

Of the initial 50 MR angiographic examinations, 10 (20%) showed flow signal in the cavernous sinus or inferior petrosal sinus or both. Flow signal was seen on nine (36%) of 25 MR angiograms obtained on scanner A and on one (4%) of 25 obtained on scanner B ($P = .02$, χ^2 analysis). The most common location of unexplained signal was in the posterior cavernous sinus, in seven of 10 cases. Four patients had MIP or source signal or both in the region of the inferior petrosal sinus. Only three patients exhibited signal of at least grade 2 on both MIP and source images (Fig 1). The length of the signal seen on the MIP images was comparable to the number of source images in which the abnormal signal was also confirmed. None of the 10 patients with cavernous sinus or inferior petrosal sinus flow signal exhibited signs or symptoms of CCF (pain, red eye, proptosis, chemosis, bruit, or ophthalmoparesis) (6, 7).

On the SE MR imaging studies, cavernous sinus signal was nonspecific in eight (80%) of 10 patients. One SE MR image showed bilateral cavernous flow voids while another showed a flow void in the right cavernous sinus. Cerebral angiograms were available for two of 10 patients. Neither demonstrated abnormal flow in the cavernous sinus or inferior petrosal sinus.

One patient's MR angiogram revealed a posterior cavernous sinus signal not identified 14 months previously on the same scanner but with different centering of the cavernous sinus in relation to the slab volume position. Another patient, found to have signal in the region of the inferior petrosal sinus suggestive of a CCF on scanner A, had no venous signal when reexamined using scanner B.

A review of the 25 patients who had both MR angiography and cerebral angiography showed that three (12%) exhibited posterior cavernous sinus signal at MR angiography. All three cerebral angiograms showed normal venous flow, and allowed no insight as to the patterns of flow that may have contributed to creating the MR angiographic flow signal.

Discussion

Relatively few studies have been published concerning the use of MR angiography in diagnosing and in following up patients with CCF. Ikawa et al (1) studied nine patients with proved CCF by conventional angiography with 3D TOF MR angiography (31–45/4.5–5.0 [TR/TE]; flip angle, 20–30°)

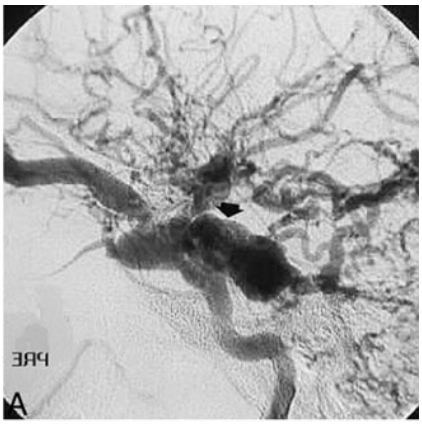

FIG 2. 12-year-old girl with chemosis, proptosis, and bruit after motor vehicle accident.

A, Right ICA arteriogram 4 months after accident shows type A direct CCF, with dilated superior-petrosal sinus-cavernous junction (*arrow*) but incomplete opacification of the inferior petrosal sinus.

B, MR angiographic source images 2 years after treatment show bilateral posterior cavernous sinus signal (*arrows*), unchanged from 1 year earlier. No clinical signs of patent CCF were present, and an arteriogram was not performed. This case illustrates the dilemma of cavernous sinus signal as a marker for CCF.

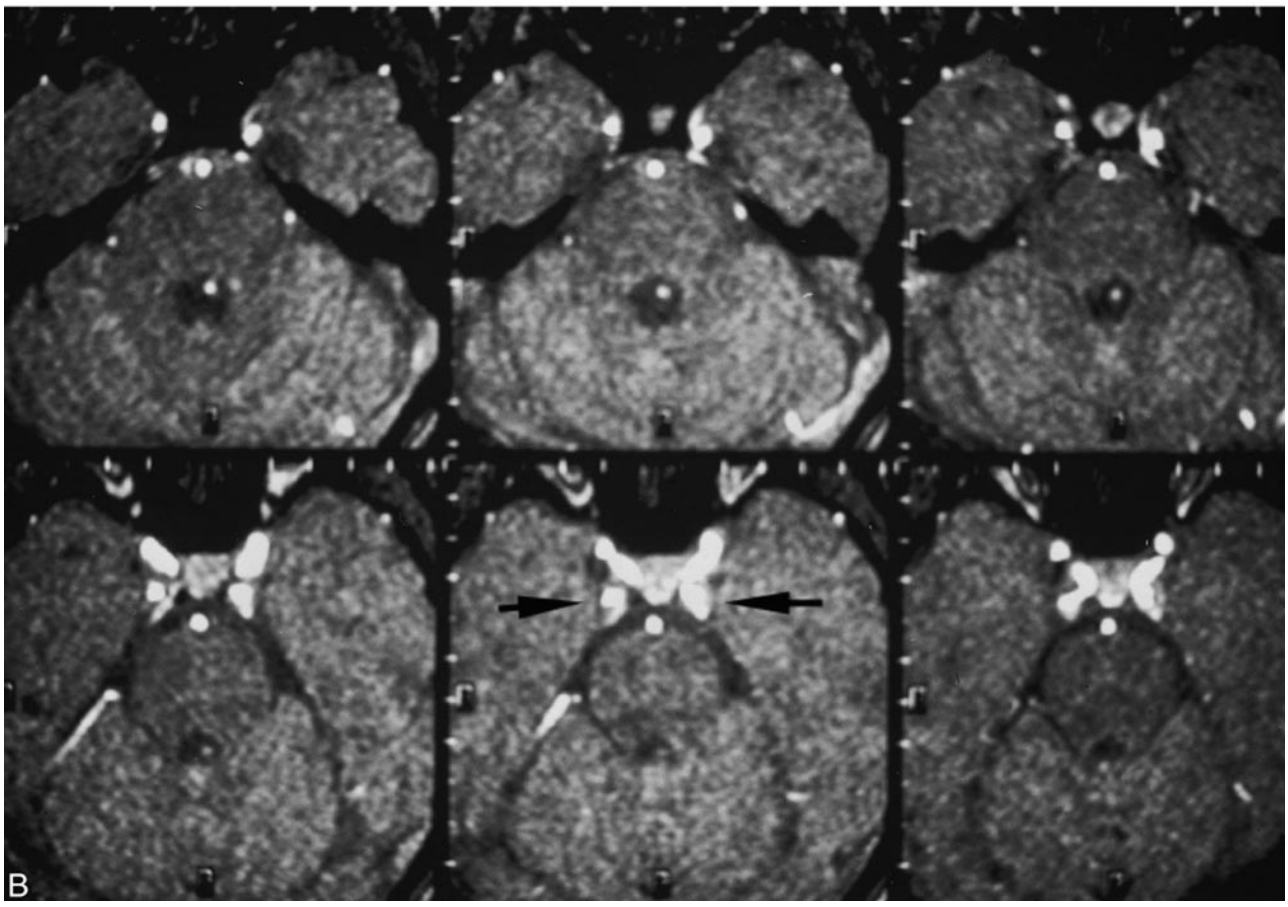

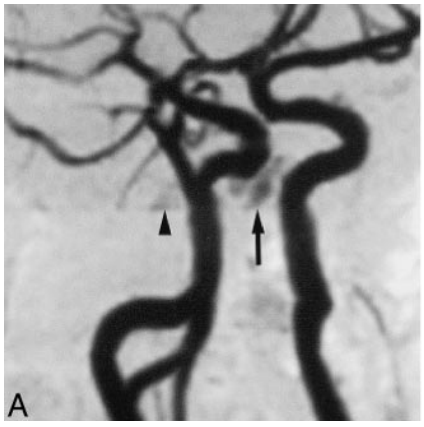

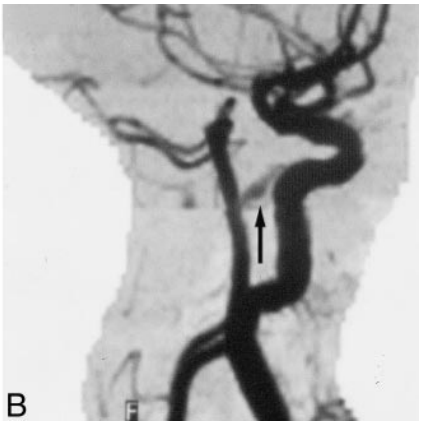

FIG 3. 81-year-old man with vertigo.

A, Oblique MIP shows bilateral (left > right) posterior cavernous sinus signal (*arrow*) and inferior petrosal sinus flow. Note saturation of flow signal at slab overlap (*arrowhead*).

B, Lateral MIP shows cavernous sinus signal (*arrow*).

Scanner parameters

	Scanner	
	A	B
TE	6.9	Min. 2.4–2.5
TR	42	35
Flip angle (FA)	20°	20°
Section thickness	1.0 mm	1.0 mm
Gap	0	0
Field of View (FOV)	17 cm	16 cm
Phase matrix	128	192
Read/frequency matrix	180	256
Phase sampling	0.883 (rectangular FOV) under sample phase matrix	100%
Signal averages/ excitations	1	1
Plane	Transverse	Axial
Phase encode	Left-right	Anterior-posterior
No. of slabs	3	3: 24 sections per slab; discard top two and bottom two sections; overlap four sections
Total sections	60 reconstructed	52 reconstructed
Presaturation	Walking presat; FA = 90°; gap = 10 mm; thickness = 60 mm	Not walking; superior; FA = 90°; gap = 10 mm; thickness = 30 mm
Magnetization transfer contrast	On: B_1 (Hz) = 800; offset (Hz) = 2500	Off
Spoiled gradient sequence	Yes	No
Flow compensation	On	Off
Ramp pulse	. . .	On Inferior → superior
Variable bandwidth	Not an option	15.63

and 3D phase-contrast techniques (26–36/7.4–10.9; flip angle, 20°; velocity-encoding gradient, 10–60 cm/s) and were able detect CCF in all nine patients by visualizing the draining veins. The most representative finding on 3D TOF MR angiography was visualization of the inferior petrosal sinus, while with 3D phase-contrast MR angiography, visualization of the superior ophthalmic vein and its reflux was the characteristic finding. Chen et al (2) studied seven patients with dural arteriovenous fistula, including one CCF, and found that TOF MR angiography (50/7; flip angle, 20°) revealed abnormal flow-related enhancement of the cavernous sinus with extension into the inferior petrosal sinus. Daniels et al (8) illustrated cavernous venous flow using gradient-echo MR imaging (100/15; flip angle, 90°) in healthy subjects.

Hirai et al (5) compared 3D fast imaging with steady-state precession (FISP) with contrast-enhanced CT and SE MR imaging in the diagnosis of CCF. Fifty-nine sides (18 in patients with CCF and 41 control studies) were evaluated. The 3D FISP MR images (20/6–7/1; flip angle, 15–20°) showed isointense signal relative to brain tissue within the cavernous sinus on all 41 control sides. The sensitivity, specificity, and accuracy in their small population sample was 83%, 100%, and 95%, respectively. The criteria used to make the diagnosis included the presence of hyperintense signal regions in or distension of the cavernous sinus or enlargement of the superior ophthalmic vein or both. Our data, however, suggest a low specificity of 3D TOF MR angiography in excluding CCF on the basis of abnormal venous signal.

Of the 75 routine 3D TOF MR angiographic studies we analyzed, 13 (17%) showed signal in the region of the inferior petrosal sinus or posterior cavernous sinus. No flow signal in the anterior cavernous sinus or superior ophthalmic vein was identified in any patient, however, which is atypical for CCF. Another important distinction from reported findings in dural arteriovenous fistulas (or Barrow type B, C, or D dural CCF, as defined, respectively, by arterial contribution from the internal carotid artery, external carotid artery, or both) was the lack of linear dural hyperintensity that is seen in dural CCFs that probably indicates the dural arteries themselves (4). The finding that more abnormal cavernous sinus/inferior petrosal sinus signal was seen on images obtained with scanner A leads us to believe that MR technique parameters may play an important role in the visualization of this normal venous signal (9–11). That venous signal is technique-related rather than disease-specific is suggested by the findings in the patient who had abnormal flow signal in the cavernous sinus region on scanner A images and subsequently had no such visible signal on scanner B images.

The vascular signal in 3D TOF MR angiography originates from the in-flow of fresh fully magne-

tized spins into the imaging volume (9–11). This in-flow enhancement is the basis for differentiating vascular structures from stationary tissue on the resulting MR angiogram. The contrast mechanism in TOF MR angiography is based on the difference in saturation between stationary tissue and flowing blood. In fact, the use of magnetization transfer contrast may increase the conspicuity of vascular signal by suppressing signal from stationary tissue more than from flowing blood, and might possibly be a factor in our observations (12).

A TR on the order of 40 milliseconds and a flip angle of 20° permit adequate visualization of in-flowing spins. A TE of 6.9 milliseconds may be used so that spins from fat and water are out of phase and thus fat signal intensity is reduced. First-order flow compensation may be employed to recover the signal loss from constant velocity flow. Motion-induced phase errors are minimized by keeping the TE as short as possible.

The greater sensitivity to venous flow exhibited by scanner A is most likely, at least in part, due to the higher TR used (42 vs 35 milliseconds). As the TR is shortened, there is progressively greater saturation of the stationary tissues. This is advantageous, up to a point, because of increased contrast between the vessel and the surrounding tissues. When TR is shortened to 35 milliseconds, however, the spins flowing through the imaging volume begin to become saturated, with resulting loss of intravascular signal intensity. For example, assuming a normal flow velocity of 30 cm/s for intracranial venous structures, at a TR of 42 milliseconds, blood will travel 12.6 mm before experiencing a second RF pulse. With a TR of 35 milliseconds, however, blood will travel only 10.5 mm before the next RF pulse. The specific flow compensation pulses used by each scanner will also affect the sensitivity to slower moving venous flow.

Flip angles can also play an important role in the signal recorded from blood flow. Like TR, the size of the flip angle determines the degree of background suppression as well as the amount of saturation of in-flowing blood. In 3D TOF, as the flip angle is decreased, there will be relatively little background saturation, but moving blood will be able to move a longer distance through its vessel without being saturated. In our study, the flip angles implemented by both scanners were the same. The use of variable (or ramped) flip angles through the imaging volume, from lower to higher flip angles in the volume, may affect background signal as well (13). Differences in MIP techniques may also create differences between two scanning instruments in flow-signal depiction. No tendency for greater conspicuity of normal venous signal in other areas was appreciated for either instrument.

Visualized flow signal in the cavernous sinus may also be related to the venous structures' position within the slab locations selected before the examination. Both scanning instruments used three overlapping slabs and reconstruction of 20 sections, centered on the pituitary fossa on midsagittal images. Cavernous sinus and inferior petrosal sinus flow signal was typically identified in the middle slab, terminating at the border with the lower slab. Termination of signal may be due to saturation-band obliteration of signal from blood flowing from superior to inferior, preventing depiction in the lower slab. Scanner A used a 60-mm-thick walking presaturation band located effectively 10 mm superiorly, and scanner B used a nonwalking 30-mm-thick band located 10 mm superiorly. On this basis, it would seem that scanner A might more effectively saturate downward venous signal with this technique, which was not the case.

It is likely that the origins of venous blood play some part in the degree of saturation and subsequent signal depiction. Flow into the anterior cavernous sinus typically arises from the superior ophthalmic veins, which have long courses parallel to the imaging axis, allowing saturation of slower-flow spins. Flow into the posterior cavernous sinus arises from the veins of the posterior fossa as well, but it is unclear what flow characteristics of these veins might contribute to the flow signal identified.

Unexplained signal suggestive of CCF can lead to unnecessary and at times invasive procedures in an effort to evaluate the abnormal finding further. The importance of the observations herein are not diminished by the time period in which the scans were performed (1996–1997) and the review completed (1998), insofar as scanner B is still operational with the same scan parameters and not infrequent demonstration of cavernous sinus flow signal.

Understanding the principles of flow depiction and the potential pitfall of a false-positive MR angiographic finding is crucial in avoiding misdiagnosis. Our analysis suggests that, in part, the unexplained signal in the cavernous sinus may be attributed to the effects of different MR parameters on the signal identified. Further work is needed to determine the exact 3D TOF MR angiographic parameters and anatomic variables that may contribute to this normal venous flow signal in the cavernous sinus and inferior petrosal sinus.

Conclusion

It is important to remember that visualization of signal in the posterior cavernous sinus or inferior petrosal sinus on 3D TOF MR angiograms may actually represent normal slow flow detected because of the preset MR angiographic parameters as well as anatomic factors. False-positive rates of up to 36% for cavernous sinus/inferior petrosal sinus venous signal as an indication of CCF may occur.

References

1. Ikawa F, Uozumi T, Kiya K, et al. **Diagnosis of carotid-cavernous fistulas with magnetic resonance angiography: demonstrating the draining veins utilizing 3-D time of flight and 3-D phase contrast techniques.** *Neurosurg Rev* 1996;19:7–12

2. Chen JC, Tsuruda JS, Halbach VV. **Suspected dural arteriovenous fistula: results of screening MR angiography in seven patients.** *Radiology* 1992;183:265–271
3. Hirabuki N, Fugita N, Hashimoto T, et al. **Follow-up MRI in dural arteriovenous malformations involving the cavernous sinus: emphasis on detection of venous thrombosis.** *Neuroradiology* 1992;34:423–427
4. Cornelius RS. **CCF: imaging evaluation.** In: Tomsick TA, ed. *Carotid-Cavernous Fistula.* Cincinnati, OH: Digital Educational Publishing 1997;23–31
5. Hirai T, Korogi Y, Ikushima I, et al. **Three-dimensional FISP imaging in the evaluation of carotid cavernous fistula: comparison with contrast-enhanced CT and spin echo MR.** *AJNR Am J Neuroradiol* 19:253–259
6. Tomsick TA. **Type A (direct) CCF: etiology, prevalence and natural history.** In: Tomsick TA, ed. *Carotid-Cavernous Fistula.* Cincinnati, OH: Digital Educational Publishing 1997;33–58
7. Tomsick TA. **Type B,C,D (dural) CCF: etiology, prevalence, and natural history.** In: Tomsick TA, ed. *Carotid-Cavernous Fistula.* Cincinnati, OH: Digital Educational Publishing 1997;59–73
8. Daniels DL, Czervionke LF, Bonneville JF, et al. **MR imaging of the cavernous sinus: value of spin echo and gradient recalled echo images.** *AJNR Am J Neuroradiol* 1988;9:947–952
9. Anderson CM, Edelman RR, Turski PA. **Time of flight angiography.** In: Clinical Magnetic Angiography. New York: Raven Press;1993:chap 2
10. Dumoulin CI, Cline HE, Souza SP, Walker MF, Wagle W. **Three-dimensional time of flight magnetic resonance angiography using spin saturation.** *Magn Reson Med* 1989;11:35–46
11. Potchen EJ, Haacke EM, Siebert JE, Gottschalk A. **Magnetic Resonance Angiography: Concepts and Applications.** St Louis, MO: Mosby;1993:380–381
12. Lin W, Tkach JA, Haacke EM, Masaryk TJ. **Intracranial MR angiography: application of magnetic transfer contrast and fat saturation to short gradient-echo, velocity compensated sequences.** *Radiology* 1993;186:753–761
13. Atkinson D, Brant-Zawadski, Gillan G, Purdy D, Laub G. **Improved MR angiography: magnetic transfer suppression with variable flip angle excitation and increased resolution.** *Radiology* 1994;190:890–894